Metabolomics in community-acquired pneumonia: exploring metabolomics-based biomarkers for diagnosis and treatment response monitoring of community-acquired pneumonia

Hartog, I. den

CHAPTER 4

Longitudinal metabolite profiling of *Streptococcus pneumoniae*-associated community-acquired pneumonia

Ilona den Hartog*, Laura B. Zwep*, Thomas Hankemeier, Jacqueline J. Meulman, Ewoudt M.W. van de Garde, J.G. Coen van Hasselt. Longitudinal metabolite profiling of Streptococcus pneumoniae-associated community-acquired pneumonia. *Metabolomics* (2024). (* Shared first authors)

Abstract

Introduction: Longitudinal biomarkers in patients with community-acquired pneumonia (CAP) may help in monitoring of disease progression and treatment response. The metabolic host response could be a potential source of such biomarkers since it closely associates with the current health status of the patient.

Objectives: In this study we performed longitudinal metabolite profiling in patients with CAP for a comprehensive range of metabolites.

Methods: Previously collected serum samples from CAP patients with confirmed *Streptococcus pneumoniae* infection (n=25) were used. Samples were collected at multiple time points, up to 30 days after admission. A wide range of metabolites was measured, including amines, acylcarnitines, organic acids, and lipids. The associations between metabolites and C-reactive protein (CRP), procalcitonin, CURB disease severity score at admission, and total length of stay were evaluated.

Results: Distinct longitudinal profiles of metabolite profiles were identified, including cholesteryl esters, diacyl-phosphatidylethanolamine, diacylglycerols, lysophosphatidylcholines, sphingomyelin, and triglycerides. Positive correlations were found between CRP and phosphatidylcholine (34:1) (cor=0.63) and negative correlations were found for CRP and nine lysophosphocholines (cor=-0.57 to -0.74). The CURB disease severity score was negatively associated with six metabolites, including acylcarnitines (tau=-0.64 to -0.58). Negative correlations were found between the length of stay and six triglycerides (TGs), especially TGs (60:3) and (58:2) (cor=-0.63 and -0.61).

Conclusion: The identified metabolites may provide insight into biological mechanisms underlying disease severity and may be of interest for exploration as potential treatment response monitoring biomarker.

4.1 Introduction

Community-acquired pneumonia (CAP) is a lower respiratory tract infection with a high incidence and is associated with the hospitalization of approximately one million adults per year [104]. The most common cause of CAP is *Streptococcus pneumoniae* [105]. In hospitalized CAP patients, there is a need to monitor the antibiotic treatment response to optimize the treatment strategy [106]. In addition, there is a need for guidance on decisions about earlier termination of antibiotic treatment to minimize the risk of antimicrobial resistance. Monitoring of treatment response is currently achieved through observation of clinical symptoms and with inflammatory markers such as C-reactive protein (CPR) and procalcitonin (PCT) [13, 12]. In particular, PCT is relevant for informing early treatment termination decisions but lacks predictive performance for CAP prognosis [107, 108]. Therefore, there is a need for biomarkers that give early insights into the clinical course of CAP.

Biomarkers that reflect the current physiological state of the patient have the potential to accurately monitor and predict the treatment response in CAP patients. Because the metabolome closely represents this physiological state, metabolomics-techniques may enable discovery of relevant novel biomarkers. Indeed, for CAP and sepsis, the potential for metabolomics-based biomarkers measured at a static time point has been demonstrated [109]. However, the longitudinal monitoring of metabolic changes within patients may allow for an improved characterization of treatment response [14]. For example, CAP patients show a change in lysophosphatidylcholines that mirrors the transition from acute illness to recovery after starting antibiotic treatment [25]. Further systematic characterization of longitudinal metabolic changes in CAP patients may thus be of relevance for identification of metabolic biomarkers that can predict and monitor the treatment response in these patients.

To this end, in this study, we aimed to comprehensively characterize the change of longitudinal metabolite profiling in hospitalized CAP patients with a confirmed *S. pneumoniae* infection using metabolomite profiling and evaluate how metabolic changes relate to disease severity based on CURB scores, established inflammation markers, and clinical treatment response quantified using the length of stay in the hospital.

4.2 Materials and methods

4.2.1 Patient cohort

We utilized serum samples collected at multiple time points during hospitalization from 25 hospitalized CAP patients with an *S. pneumoniae* infection. These samples were previously collected as part of a larger clinical study that was performed between November 2007 and September 2010 [29]. The causative pathogen was identified

using culturing or a urinary antigen test. We selected samples from patients with a confirmed *S. pneumoniae* infection. We excluded patients with a mixed infection involving additional pathogen(s) and one patient that died during the study period. Samples were collected at five time points: at the day of admission (day 0), and at days 1, 2, 4, and 30 after admission. CRP and creatinine were measured in the hospital at the same time points as the blood samples used for metabolite profiling obtained. Samples were stored at -80 degrees Celsius, and went through a maximum of 2 freeze-thaw cycles, so stable metabolites were preserved in the samples [110, 111]. Not all time points were available for each patient, resulting in 115 samples over the 25 patients. On the day of admission, disease severity was determined using the CURB score, which is a scoring system based on confusion, blood urea > 7 mmol/l, respiratory rate (RR) $\geq$ 30/min; systolic BP < 90 mmHg or diastolic BP $\leq$ 60 mmHg [112]. A score of two or higher is classified as severe CAP.

4.2.2 Bio-analytical procedures

Serum samples were analyzed using five targeted LCMS methods and one targeted GCMS method by the Biomedical Metabolomics Facility of Leiden University, Leiden, The Netherlands, as described previously [59]. The metabolomics profiling covered 596 metabolite targets from 25 metabolite classes, including amino acids, biogenic amines, acylcarnitines, organic acids, and multiple classes of lipids. Details of the metabolomic analysis methods used are provided in section 4.5. A total of 369 unique metabolites was measured as relative levels, of which 6 metabolites were removed due to high missingness ($\geq$ 20%), resulting in 363 metabolites being evaluated in data analysis. Biochemically-selected sums and ratios of metabolites were calculated and added to the data (Table 4.2).

PCT was measured in the same serum samples used for the metabolomite profiling analysis. PCT analysis was performed using the human procalcitonin CLIA kit from Abbexa (abx190129). Samples were measured in duplicate if sample volumes were sufficient (95% of samples).

4.2.3 Data analysis

The metabolite levels were scaled through log-transformation and standardization. To explore the variability of the high-dimensional metabolomite profiling dataset, principal component analysis (PCA) was used. The PCA was used on the scaled metabolite profiling data over the different time points, with the metabolites as variables and each observation being a sample from a patient for a specific time point [113]. As part of the PCA, missing values were imputed through multiple imputation using expectation maximization (EM-PCA), which iteratively calculates the principal components and imputes the missing values [114].

To evaluate how much of the variation in the metabolites could be explained by the change over time, the first two principal components were related to time using a

polynomial regression model. The importance of the metabolites to explain the variation between the patients over time was evaluated by evaluating the squared variable loadings. Specifically, the squared variable loadings within and between biochemical metabolite classes were evaluated to study similarities within classes and see which biochemical classes vary more between the patients.

To characterize the metabolic time profiles and profiles of current inflammation markers for different patients, we estimated the correlations between the scaled metabolite levels and CRP, PCT and creatinine levels over time. Next, we evaluated which metabolites could be of interest for the prediction of the clinical course, by estimating the Kendall's Tau correlation between the scaled metabolite levels and a clinical disease severity marker, the CURB score [112] at hospital admission, and estimating Pearson correlation between the scaled metabolite levels and the outcome length of stay (LOS) in the hospital. Since the CURB and LOS are static values, while the metabolites changed over time, the correlations between these outcomes and the change in metabolite levels from baseline ($m_{t=k}$ - $m_{t=0}$) at each time point (k) were calculated. Due to the large number of correlations calculated and the small sample size, the correlations were not tested for significance, to prevent multiple testing problems. In our analysis we focused on metabolites with the largest (positive or negative) correlation, as exploratory analysis. The metabolites with the largest correlations were further evaluated in literature research to assess their biological function.

All analyses were performed in R. The scripts used for the analyses were deposited on GitHub (http://github.com/vanhasseltlab/LongitudinalMetabolomicsCAP/tree/manuscript).

4.3 Results

4.3.1 Metabolite time profiles

Metabolite profiling was performed for 25 patients and resulted in 363 metabolite levels on five time points (Table 4.3). The patient characteristics are displayed in Table 4.1. Comorbidities present in patients included kidney disease (n = 1), cardiovascular disease (n = 4), malignancy (n = 2), COPD (n=1, $n_{missing}$ = 15), diabetes (n=3, $n_{missing}$ = 15). No patients were using corticosteroids before admission ($n_{missing}$ = 15).

Metabolite profiles within all CAP patients shifted over time, as shown in the PCA over all time points (Figure 4.1). The close relationship between metabolite levels and time is reflected in the results from the polynomial regression model which indicated that 45% of the metabolite variation captured in these first two principal components could be explained by time. Due to the large age range, we tested whether age was a large explanatory factor for the metabolite differences between individuals, but did not find a significant contribution of age (section 4.5).

Table 4.1 Patient characteristics

Patient characteristics	CAP patients (n=25)
Age (years)	
Median [Min, Max]	67.0 [18.0, 98.0]
Sex	
Male	12 (48.0%)
Female	13 (52.0%)
CURB score	
Median [Min, Max]	1.00 [0, 3.00]
Duration of symptoms before admission (days)	
Median [Min, Max]	3.00 [1.00, 14.0]
Missing	15 (60.0%)
Antibiotic treatment before admission	
No	8 (32.0%)
Yes	2 (8.0%)
Missing	15 (60.0%)
Length of stay (days)	
Median [Min, Max]	7.50 [2.50, 24.5]

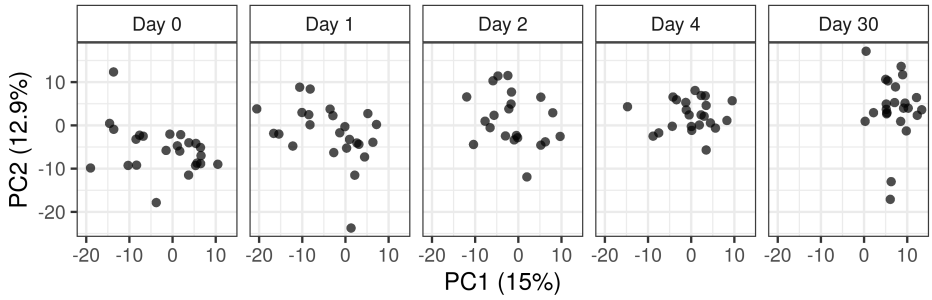

Figure 4.1 PCA scores for patient metabolite profiles over time. Every point represents the scores of an individual patient at a certain time point, in two dimensions based on the metabolite values. The panels show a trend over time of the metabolite profiles.

The metabolites that were targeted in this study were categorized into different biochemical classes. Metabolites from different biochemical classes showed distinct contributions to the total variation between the patients over time as was expressed in the variable loadings and directionality of the principal components (Figure 4.2). The squared PCA loadings represent the weight that the different metabolites in the biochemical class have in explaining the variation between patients over time. Of the variation in principal component one and two, 48% was explained by metabolites of the classes of cholesteryl esters, LPC's, sphingomyelins, diacylglycerols, and triglycerides (Figure 4.2A). The metabolites were categorized in classes based on their biochemistry and not based on their biological functions. The PCA indicate that metabolites that are categorized in the same class do not necessarily behave similarly (Figure 4.2B). For example, amino acids behave very differently from each other. Metabolites that do behave similarly in their biochemical class are for example triglycerides and sphingomyelins.

For each patient, the metabolic time profiles were shown as the two first components from the PCA (Figure 4.3, Figure 4.7). Generally, a shift from low to high principal component values was seen over time, corresponding to the shift in metabolite levels for the different metabolites (Figure 4.2B). The large variability in the time profiles indicates a large interpatient variability in metabolic levels and changes over time.

4.3.2 Inflammation marker associations

To explore associations between metabolite profiles and inflammation, the metabolite values were compared to currently used inflammation biomarkers. Correlations were found between CRP and PCT and several metabolites. For example, phosphocholine (PC) (34:1) showed a positive correlation with CRP (cor = 0.63). Several individual lysophosphocholines (LPCs) and the sum of all LPCs showed a negative correlation with CRP (cor = -0.57 to -0.74, Figure 4.4A). PC (34:1) was found to decrease over time and several LPCs showed an increase over time, thereby mirroring the clinical disease progression (Figure 4.4B). Positive correlations with CRP and PCT were reported for the short-chain acylcarnitines (SCACs) tiglylcarnitine, 2-methylbutyroylcarnitine, and isovalerylcarnitine (cor with PCT = 0.61, 0.58, and 0.57; cor with CRP = 0.54, 0.64, and 0.51, respectively). Negative correlations were seen between the long-chain acylcarnitine (LCAC) stearoylcarnitine and CRP (cor = 0.62). This trend for decreasing SCACs over time is also represented by the positive correlation of CRP and PCT with the sum of all SCACs (cor = 0.55 and 0.53, respectively).

Correlations between metabolite levels and creatinine, a marker of renal failure, were also identified. The same trends were seen for creatinine as for CRP and PCT (Figure 4.8). Strong positive correlations were observed between creatine and 1-Methylhistidine, SDMA, inositol, homoserine, methionine sulfone, and octanoylcarnitine (cor > 0.7)

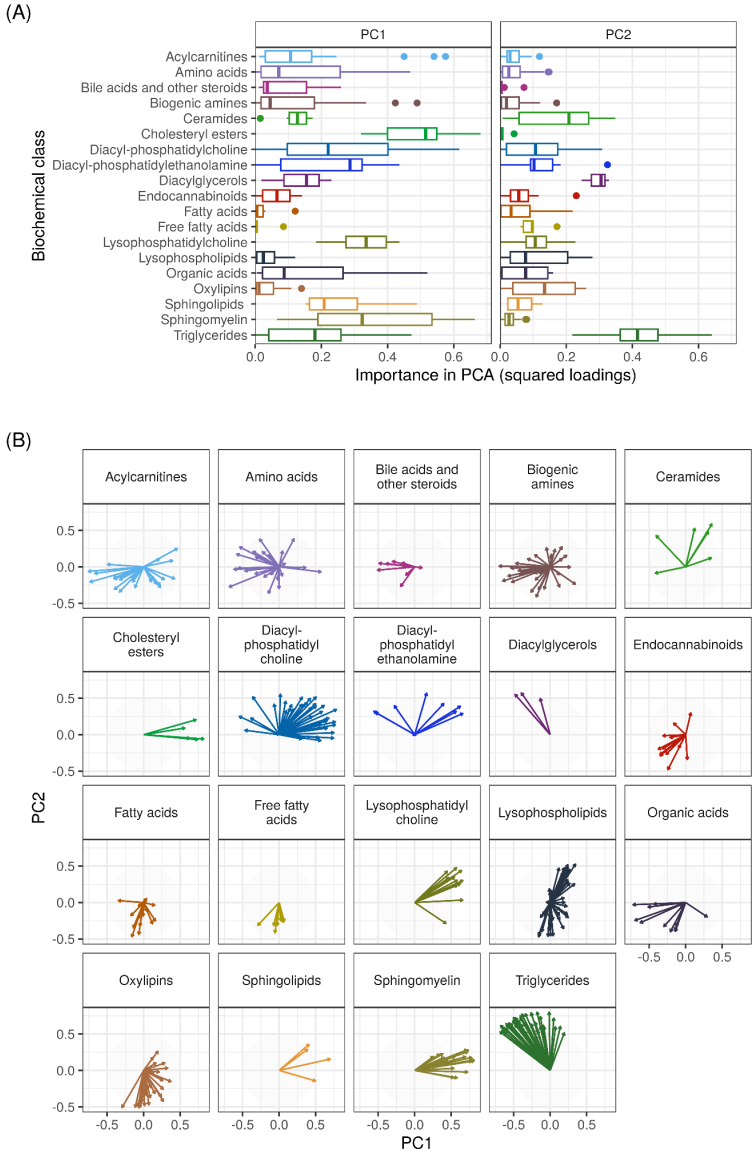

Figure 4.2 Metabolite contributions to the two dimensions of the PCA as variable loadings. a) The importance of each biochemical class for the different principal components (PCs), expressed by their squared metabolite loadings. Each box represents the squared loadings of the metabolites within a metabolic class. High squared loadings indicate a larger contribution to explaining the variation between patients. b) The loading plots for each biochemical metabolite class. The arrows indicate the importance (length) and direction of the metabolites in the principal component space. For example, high PC1 values correspond to high metabolite levels for metabolites with right pointing arrows, and low metabolite levels for metabolites with left pointing arrows. Arrows with a similar direction have similar metabolite patterns. Abbreviations: PC: principal component.

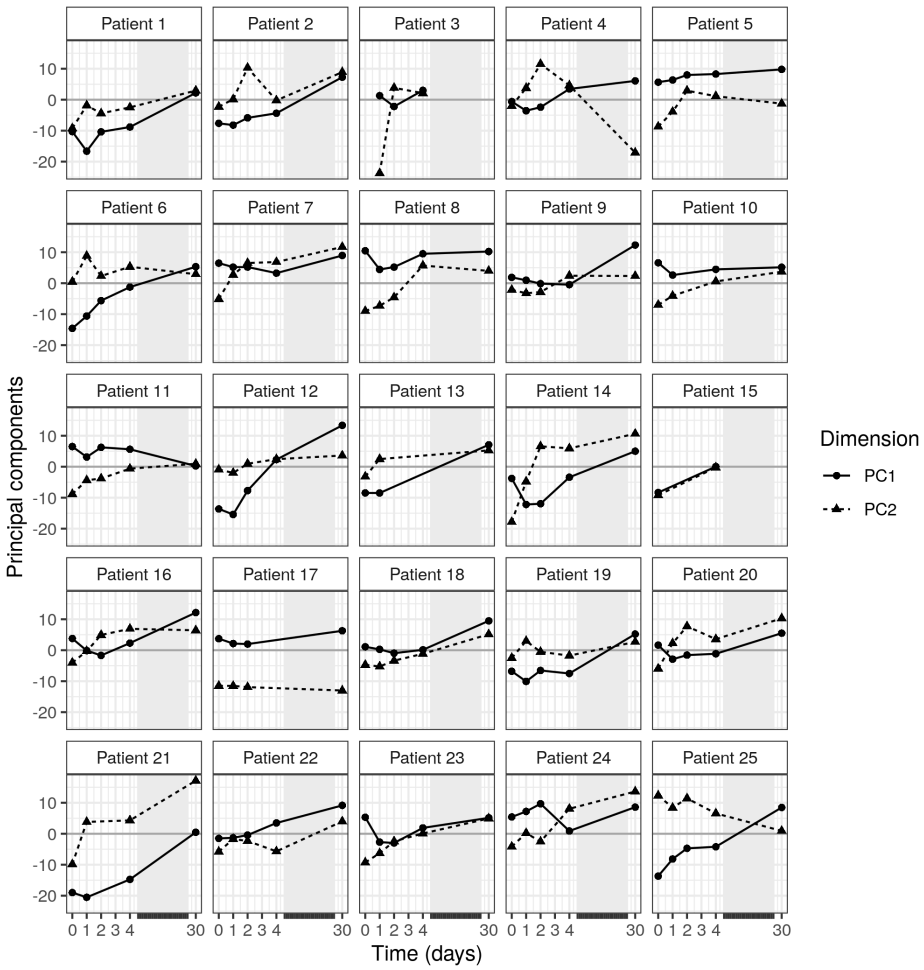

Figure 4.3 Individual time profiles over PC1 and PC2. The lines PC1 (solid) and PC2 (dashed), indicate the change in the corresponding principal component over time. Changes in PC values correspond to changes in metabolite levels according to their respective loadings. Abbreviations: PC: principal component. Abbreviations: PC: principal component.

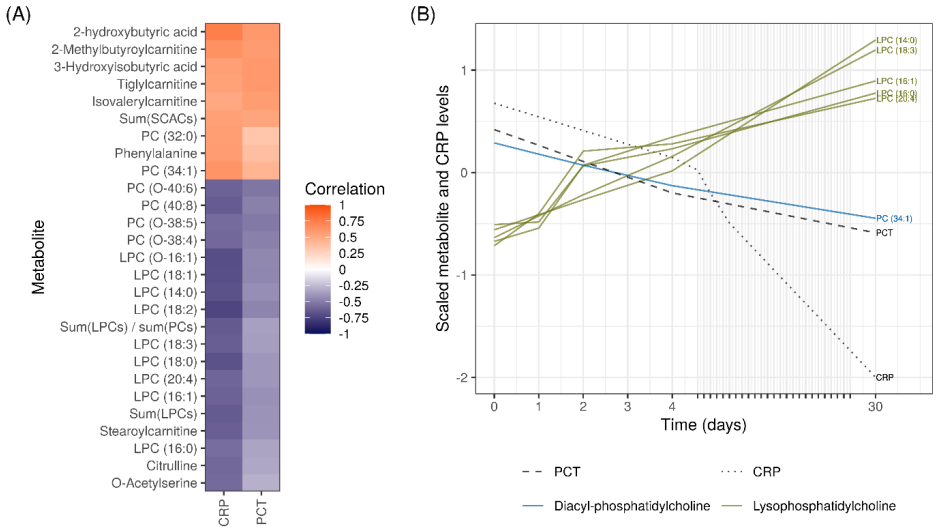

Figure 4.4 Correlations between inflammation markers CRP and PCT, and metabolites. A) The correlations between metabolites and CRP or PCT. Metabolites with a correlation >0.55 or <-0.55 for at least one marker are shown. A positive correlation (orange) indicates that a higher CRP or PCT level corresponds to an increase of that metabolite over time, while a negative correlation (blue) indicates a decrease over time for patients with a higher CRP or PCT level. B) Average CRP, PCT, PC (34:1), and LPC levels over time over all patients. Metabolite and CRP data were scaled. Abbreviations: see the abbreviation list.

4.3.3 Disease severity score associations

To identify possible metabolic biomarkers for indication of disease severity, associations between the CURB disease severity score at admission and the change in metabolite levels on from day 0 to days 1, 2, 4, and 30 were evaluated (Figure 4.8). Negative associations were found between the CURB score and the change of metabolite levels (m) between day 0 and day 30 ($m_{t=30} - m_{t=0}$) of tiglylcarnitine, isovalerylcarnitine, 3-hydroxyisovaeric acid, carnitine, N6,N6,N6-trimethyl-lysine, and isobutyryl carnitine (tau = -0.64 to -0.58, Figure 4.5). Patients with higher CURB scores showed decreasing levels of these metabolites.

4.3.4 Hospital length of stay associations

We evaluated the association between metabolites and clinical outcomes using the length of stay (LOS) as a potential surrogate endpoint. The strongest negative correlations to LOS were reported for the metabolite change over the first two days of admission ($m_{t=2} - m_{t=0}$, Figure 4.6), especially for the triglycerides (TGs) (60:3) and (58:2) (cor = -0.63 and -0.61 respectively). The correlations of these metabolites to LOS were much stronger than to CRP and PCT (cor = -0.08 and -0.25 respectively). Positive

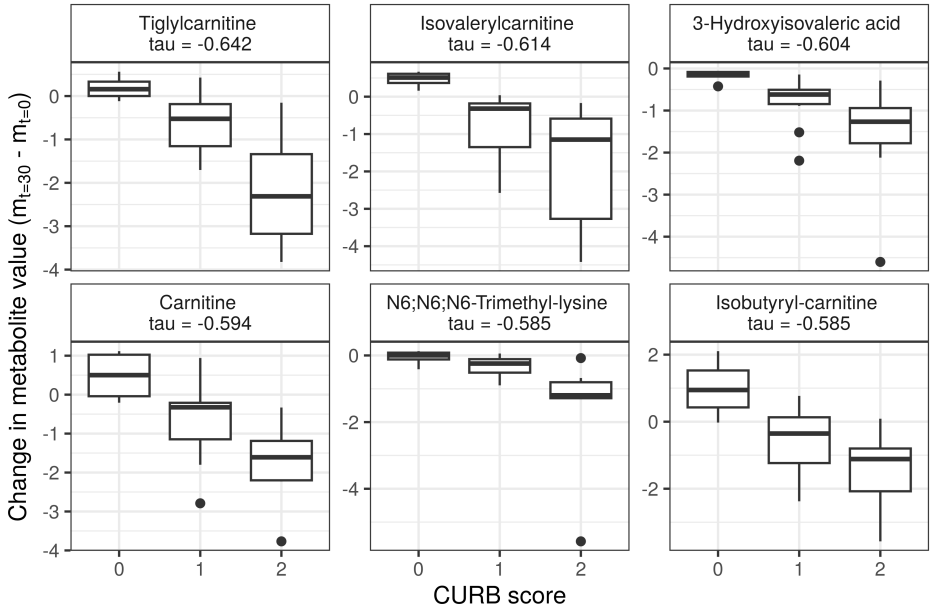

Figure 4.5 The correlation between the CURB score and six metabolites with highest associations. The change in metabolite level is the difference between the scaled metabolite level at day 30 and scaled metabolite level at admission (y-axis). These six metabolites all show a negative correlation with the CURB score (tau). This means, for patients with a CURB score of 0 the metabolite change between day 30 and day 0 is positive, so their metabolite levels were increasing over time. For patients with a CURB score of 2, the metabolite levels decreased over time.

correlations were most pronounced when analyzing the metabolite change from the day of admission to day 30 ($m_{t=30} - m_{t=0}$). In the case of fatty acid (FA) (22:1) the day after admission ($m_{t=1} - m_{t=0}$) was the most strongly positively correlated to the LOS (cor = 0.58).

4.4 Discussion

In this study, we characterized the dynamics of the serum metabolites in pneumococcal CAP patients. We found that a large part of the variation in the metabolite values was associated with time-varying changes in metabolites within the patients. We furthermore found that several groups of metabolites were found to correlate with inflammation markers, CURB score, and length of hospital stay. These findings both support the potential relevance of metabolite-based biomarkers to monitor the treatment response or disease progression in CAP.

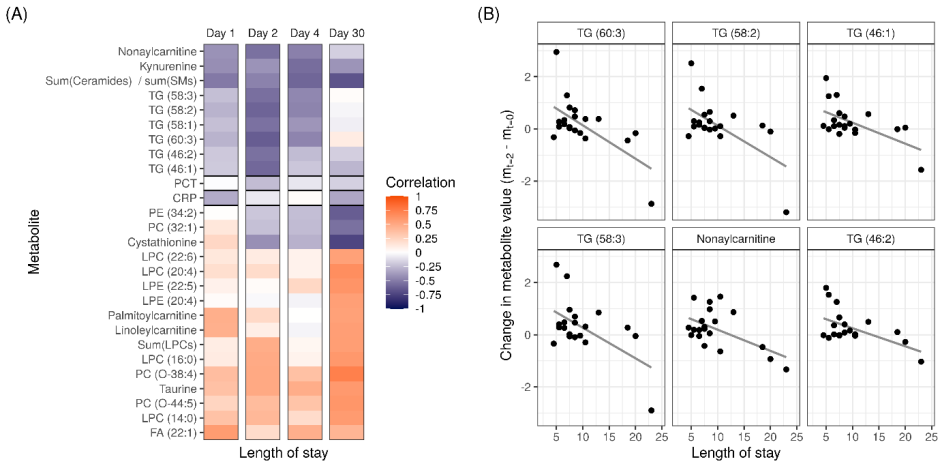

Figure 4.6 a) The correlations between the length of stay and metabolite change from baseline at days 1, 2, 4, and 30 after admission ($m_{t=k}$ - $m_{t=0}$). CRP and PCT are added as a reference. A positive correlation (orange) indicates that a longer stay in the hospital corresponds to an increase of that metabolite over time, while a negative correlation (blue) indicates a decrease over time for patients with longer stay. b) Metabolite levels over time for individual patients for metabolites with large negative correlations (cor < -0.55) over the first two days after admission. Abbreviations: see the abbreviation list.

We found that length of stay in the hospital was negatively correlated with the triglycerides TG (60:3) and TG (58:2). . Interestingly, these TGs are not highly correlated to CRP, PCT, or the CURB score, which suggests that they can explain a part of the variability of disease progression in patients not explained by established biomarkers for inflammation. We previously found that TGs do not contribute to the etiological prediction of pathogenic in CAP [59]; as such TGs may be of interest as potential biomarker beyond pneumococcal CAP studied in this analysis. Further studies should however consider the potential impact of diet on TGs, as a potential confounding factor [115].

Phosphatidylcholine (PC) (34:1) and lysophosphatidylcholines (LPCs) (14:0), (16:0), (16:1), (18:0), (18:1), (18:2), (18:3) and (20:4) correlated to inflammatory markers, which also corresponds to previous findings [25, 116]. PC (34:1), a ligand of nuclear receptor PPARα30, showed a positive correlation with CRP, which was previously associated with an anti-inflammatory response [117]. LPC 14:0 has been recently identified as a biomarker for disease severity in CAP patients [118]. Due the correlation with CRP, these metabolites could be of interest as treatment response biomarkers, also beyond pneumococcal CAP patients [34].

The CURB score was negatively associated with six metabolites, including several acylcarnitines. One of these acylcarnitines, tigylcarnitine, has previously been found

to be increased in non-survivors of CAP and could be considered a marker for disease severity [116]. Isovalerylcarnitine and isobutyrylcarnitine have, to our knowledge, not been studied as disease severity marker before, but may show a comparable performance to tigylcarnitine as their direction on the first principal component is similar.

In this analysis we demonstrated which biochemical metabolite classes explain most of the variation in metabolite patterns between individuals and over time. Triglycerides and LPCs were important for explaining the variation over time in the principal component analysis (PCA) and correlated with LOS and inflammatory markers. Within the biochemical classes, not all metabolites showed similar patterns, indicating that metabolites in some biochemical classes behave similarly during the infection, while metabolites in other classes behave differently (Figure 4.2B). The amino acids behave very differently, which could be expected since they are involved in a wide variety of biological functions [119].

The longitudinal analysis of the metabolomite profiling data enabled us to gain insight into acute and longer-term changes in the metabolome during the clinical course of CAP. Since patients are admitted to the hospital in different stages of the disease, interpretation of the metabolite profile at one time point can be challenging. The longitudinal metabolite profiles that were measured in this study give more information about the state of the patient and elucidate the effect of comorbidities and co-medications. The principle component analysis (Figure 4.3) showed large variability between different patients, indicating the importance of considering changes within patients, instead of evaluating the metabolite profile at one timepoint. We found that the differences in metabolite levels were largely explained by changes over time and were, therefore, related to the treatment response.

This study was conducted in a well-characterized set of CAP patients with *S. pneumoniae* infections. *S. pneumoniae* is a common cause of CAP, but other bacterial or viral pathogens can also be the cause of CAP. A previous study did not show significant differences in metabolic profiles between common causes of CAP [59]. The results of the current study may apply to CAP patients with these other causative pathogens, but this is still unsure because the previous study does not cover changes over time. Especially metabolites associated with length of stay should be validated in CAP cohorts with various causative pathogens, since they are not related to the general inflammatory response.

In further research, the addition of patients with other causes of CAP is of interest to compare metabolic time profiles for different treatment strategies based on the causative pathogen. Early recognition of a pathogen-drug mismatch using metabolite profiling could make antibiotic therapies more targeted and shorter. This study shows that mainly TGs, LPCs, PCs, and acylcarnitines are of interest for the disease severity and the length of stay for patients with CAP. By focusing on these metabolite classes, the number of metabolites that has to be measured for every patient can be reduced.

In conclusion, we find that that metabolomics-based biomarkers have potential for treatment response monitoring in CAP patients. The triglycerides found in this study could potentially complement the currently available biomarkers such as CRP and PCT as they yield additional information about the clinical course in these patients. This study furthermore supports the relevance for collecting longitudinal data to follow the highly dynamic metabolite profiles in patients, which can further enable the development of personalized treatment strategies.

4.5 Supplementary Information

Details on metabolite profiling methods

Batch design: Aliquoted samples were run in a randomized fashion in several batches together with quality control (QC) samples (every 10 samples), sample replicates (every 7 samples), internal standards (ISTDs), blanks, and calibration lines.

Quality control: Blank samples were used to determine the blank effect. Replicate samples were used to check the instrument for repeatability. In-house developed algorithms were applied using the pooled QC samples to compensate for shifts in the sensitivity of the mass spectrometer over the batches.

Reported results: After quality control correction the metabolites that complied with the acceptance criteria of a relative standard deviation of the quality control samples (RSDqc) <15% were reported. The data was reported as relative response ratio (analyte signal area / ISTD area; unit free) of the metabolites after QC correction. Metabolites that did not comply with the acceptance criteria of the quality control, but have been included in the results present RSDs up to 30% and should be handled with caution.

Amine profiling : Amine profiling was performed according to the validated amine profiling analytical platform with minor optimization [50] . The amine platform covers amino acids and biogenic amines employing an Accq-Tag derivatization strategy adapted from the protocol supplied by Waters. 5,0 μL sample was spiked with an internal standard solution. Protein precipitation was performed by addition of MeOH and the sample was dried in a speedvac. The residue was reconstituted in borate buffer (pH 8.5) with AQC reagent. The prepared samples were transferred to autosampler vials and placed in an autosampler tray. The vials were cooled at 4^{o} C upon injection. 1,0 μL prepared sample was injected in a UPLC-MS/MS system. Chromatographic separation was achieved by an Agilent 1290 Infinity II LC System on an Accq-Tag Ultra column (Waters) with a flow of 0.7 mL/min over an 11 min gradient. The UPLC was coupled to electrospray ionization on a triple quadrupole mass spectrometer (AB SCIEX Qtrap 6500). Analytes were detected in the positive ion mode and monitored in Multiple Reaction Monitoring (MRM) using nominal mass resolution. Acquired data was evaluated using MultiQuant Software for Quantitative Analysis (AB SCIEX, Version 3.0.2), by the integration of assigned MRM peaks and normalization using proper

internal standards. For analysis of amino acids, their 13C15N-labeled analogs were used. For other amines, the closest-eluting internal standard was employed. After quality control correction the amines that complied with the acceptance criteria of RSDqc <15% were included in the results. Additionally, the amines that presented an RSDqc between 15 and 30% were included in the results but these compounds should be considered with caution.

Acylcarnitine profiling: The acylcarnitine platform covers acylcarnitines as well as trimethylamine-N-oxide, choline, betaine, deoxycarnitine, and carnitine. 10 μL sample was spiked with an internal standard solution. Protein precipitation was performed by addition of MeOH. The supernatant was transferred to an autosampler vial and placed into an autosampler. The vials were cooled at 10°C upon injection. 1.0 μL of the prepared sample was injected into a triple quadrupole mass spectrometer. Chromatographic separation was achieved by UPLC (Agilent 1290, San Jose, CA, USA) on an Accq-Tag Ultra column (Waters) with a flow of 0.7 mL/min over an 11 min gradient. The UPLC was coupled to electrospray ionization on a triple quadrupole mass spectrometer (Agilent 6460, San Jose, CA, USA). Analytes were detected in the positive ion mode and monitored in Multiple Reaction Monitoring (MRM) using nominal mass resolution. Acquired data was evaluated using Agilent MassHunter Quantitative Analysis software (Agilent, Version B.05.01), by integration of assigned MRM peaks and normalization using proper internal standards. The closest-eluting internal standard was employed. After quality control correction the compounds that complied with the acceptance criteria of RSDqc <15% were included in the results. Additionally, the compounds that presented an RSDqc between 15 and 30% were included in the results but these compounds should be considered with caution.

Organic acid profiling: The organic acid platform covers 28 organic acids. 50 μL sample was spiked with an internal standard solution. Protein precipitation was performed by addition of MeOH. After centrifugation, the supernatant was transferred and the sample was dried using a speedvac. Then, two-step derivatization procedures were performed on-line: oximation using methoxyamine hydrochloride (MeOX, 15 mg/mL in pyridine) as the first reaction and silylation using N-Methyl-N-(trimethylsilyl)- trifluoroacetamide (MSTFA) as the second reaction. 1 μL of each sample was directly after its derivatization injected on GC-MS. Gas chromatography was performed on an Agilent Technologies 7890A equipped with an Agilent Technologies mass selective detector (MSD 5975C) and MultiPurpose Sampler (MPS, MXY016-02A, GERSTEL). Chromatographic separations were performed on an HP-5MS UI (5% Phenyl Methyl Silox), 30 m × 0.25 m ID column with a film thickness of 25 μm, using helium as the carrier gas at a flow rate of 1,7 mL/min. A single-quadrupole mass spectrometer with electron impact ionization (EI, 70 eV) was used. The mass spectrometer was operated in SCAN mode mass range 50-500. Acquired data was evaluated using Agilent MassHunter Quantitative Analysis software (Agilent, Version B.05.01). After quality control correction and considering blank effects, the organic acid compounds that complied with the acceptance criteria RSDqc <15% and blank effect

<20% were included in the results. Also, the organic acids that reported an RSDqc between 15 and 30% were included and should be considered with caution.

Negative lipid profiling: The negative lipid platform is a semi-target methodology for the identification of 30 fatty acids. 50 µL sample was spiked with 50 μL of an internal standard solution. Protein precipitation was performed by addition of 550 μL MeOH. After centrifugation, 600 μL supernatant was transferred and the sample was dried using a speedvac. The residue was reconstituted in 300 μL of isopropanol with 0,1% formic acid. The prepared samples were transferred to autosampler vials and placed in an autosampler tray. 8,0 µL of the prepared sample was injected into an LC-MS. The analysis was performed on an ACQUITY UPLC™ (Waters, the Netherlands) coupled to a high-resolution mass spectrometer with a Synapt G2 Q-TOF system (Waters, the Netherlands) using reference lock mass correction. Lipids were detected in full scan in the negative ion mode. Chromatographic separation was achieved using an HSS T3 column (1.8 µm, 2.1 * 100 mm) with a flow of 0.4 mL/min over a 16-minute gradient. Acquired data was preprocessed using Targetlynx software (Masslynx, V4.1, SCN916). After quality control correction, the compounds that complied with the acceptance criteria RSDqc <15% were included in the results. Additionally, the compounds that reported an RSDqc between 15 and 30% were included in the results and should be considered with caution.

Positive lipid profiling: The positive lipid platform covers 185 compounds including triglycerides (TGs, n=85) and non-triglycerides (non-TGs, n=100). 10 µL preprocessed sample was spiked with 1000 µL IPA containing internal standards and vortexed for 30 sec. Prepared samples were transferred to autosampler vials for LC-MS analysis. In total 2.5 µL prepared sample was injected for analysis. Chromatographic separation was achieved on an ACQUITY UPLC™ (Waters, Ettenleur, the Netherlands) with an HSS T3 column (1.8 µm, 2.1 * 100 mm) with a flow of 0.4 mL/min over a 16 min gradient. The lipid analysis is performed on a UPLC-ESI-Q-TOF (Agilent 6530, Jose, CA, USA) high-resolution mass spectrometer using reference mass correction. Lipids were detected in full scan in the positive ion mode. The raw data were preprocessed using Agilent MassHunter Quantitative Analysis software (Agilent, Version B.04.00). After quality control correction, the TGs and non-TGs compounds that complied with the acceptance criteria RSDqc <15% and blank effect <40 % were included in the results. The TG and non-TGs that reported an RSDqc between 15 and 30% were also included and should be considered with caution.

Signaling lipid profiling: The signaling lipids platform covers various isoprostane classes together with their respective prostaglandin isomers from different poly unsaturated fatty acids (PUFA), including n-6 and n-3 PUFAs such as dihomo-γ-linoleic acid (DGLA) and arachidonic acid (both n-6) and eicosapentaenoic acid (EPA) and docosahexaenoic acid (DHA) (both n-3). Also included in this platform are endocannabinoids, bile acids, and signaling lipids from the sphingosine and sphinganine classes and their phosphorylated forms, as well as three classes of lysophosphatidic acids. The three lysophosphatidic acid classes include lysophosphatidic acids (LPAs),

lysophosphatidylglycerol (LPG), lysophosphatidylinositol (LPI), lysophosphatidyserine (LPS), lysophosphatidylethanolamines (LPE), cyclic-phosphatidic acids(cLPA), and fatty acid all ranging from C14 to C22 chain length species. The signaling and peroxidized lipids platform is divided into two chromatographic methods: low and high pH. In the low pH method, isoprostanes, prostaglandins, nitro-fatty acids, lyso-sphingolipids, endocannabinoids, and bile acids are analyzed. The high pH method covers lyso-sphingolipids, lysophosphatidic acids, lysophosphatidylglycerol, lysophosphatidylinositol, lysophosphatidyserine, lysophosphatidylethanolamines, cyclic-phosphatidic acids, and fatty acid. Each sample was spiked with antioxidant and internal standard solution. The extraction of the compounds is performed via liquid-liquid extraction (LLE) with butanol and methyl tert-butyl ether (MTBE). After collection, the organic phase is concentrated by first drying followed by reconstituted in a smaller volume. After reconstitution, the extract is transferred into amber autosampler vials and used for high and low pH injection. A Shimadzu system, formed by three high-pressure pumps (LC-30AD), a controller (CBM-20Alite), an autosampler (SIL-30AC), and an oven (CTO-30A) from Shimadzu Benelux, was coupled online with an LCMS-8050 triple quadrupole mass spectrometer (Shimadzu) for high pH measurements. An LCMS-8060 triple quadrupole mass spectrometer (Shimadzu) was coupled to the Shimadzu system for low pH measurements. Both systems were operated using LabSolutions data acquisition software (Version 5.89, Shimadzu). The samples were analyzed by UPLC-MS/MS. An Acquity UPLC BEH C18 column (Waters) was used to measure the samples in the low pH method. For the high pH method, a Kinetex EVO column by Phenomenex was used. The triple quadrupole mass spectrometer was used in polarity switching mode and all analytes were monitored in dynamic Multiple Reaction Monitoring (dMRM). The acquired data was evaluated using LabSolutions Insight software (Version 3.1 SP1, Shimadzu), by integration of assigned MRM peaks and normalization using accordingly selected internal standards. When available, a deuterated version of the target compound was used as an internal standard. For the other compounds, the closest-eluting internal standard was employed. For low pH mode, after quality control correction, the metabolites that complied with the acceptance criteria of RSDqc <15% and blank effect <40% were included in the results. Additionally, the compounds that reported an RSDqc between 15 and 30% were included in the results and should be considered with caution. For high pH mode, after quality control correction, the metabolites that complied with the acceptance criteria of RSDqc <15% and blank effect <40% were included in the results. Additionally, the compounds that reported an RSDqc between 15 and 30% were included in the results and should be considered with caution.

Testing the influence of age on metabolite profiles

To test whether the age is a factor to take into account in the correlation analysis between the change in metabolite values and the CURB score and hospitalization time, we tested the whether the interindividual variance of the metabolite profiling was explained by age, to decide whether age should be a confounder in the analysis. To test this, we did an anova test to compare a mixed effect model on the principal components, which

represent the metabolite profiles in a lower dimension, in two models: one with only an patient specific random effect and one model that included both a patient specific random effect and a parameter for age. The anova was done two times, with the first and second principle component scores as outcomes respectively. The code and outcomes of the anova are shown below, where subject.id denotes the patient and age is the age variable. The p-values for principle component 1 and 2 were 0.18 and 0.09 respectively and did not indicate a significant improvement of the model including age over the model not including age, which motivated the correlation analysis without adding age as confounder or using it to stratify the analysis. The small sample size could be a reason for not finding significance, but this is also a reason for not stratifying the analysis.

```
lmer_age_pc1 <- lmer(PC1 ~ age + (1|subject.id),
                data = pca_data, REML = F)
lmer_pc1 <- lmer(PC1 ~ (1|subject.id),
            data = pca_data, REML = F)
anova(lmer_pc1, lmer_age_pc1)

             npar    AIC    BIC  logLik deviance  Chisq Df Pr(>Chisq)
lmer_pc1        3 768.60 776.83 -381.30   762.60
lmer_age_pc1    4 768.82 779.80 -380.41   760.82 1.7827  1     0.1818

lmer_age_pc2 <- lmer(PC2 ~ age + (1|subject.id),
                data = pca_data, REML = F)
lmer_pc2 <- lmer(PC2 ~ (1|subject.id),
            data = pca_data, REML = F)
anova(lmer_pc2, lmer_age_pc2)

             npar    AIC    BIC  logLik deviance  Chisq Df Pr(>Chisq)
lmer_pc2        3 770.96 779.19 -382.48   764.96
lmer_age_pc2    4 770.10 781.08 -381.05   762.10 2.8589  1    0.09087
```

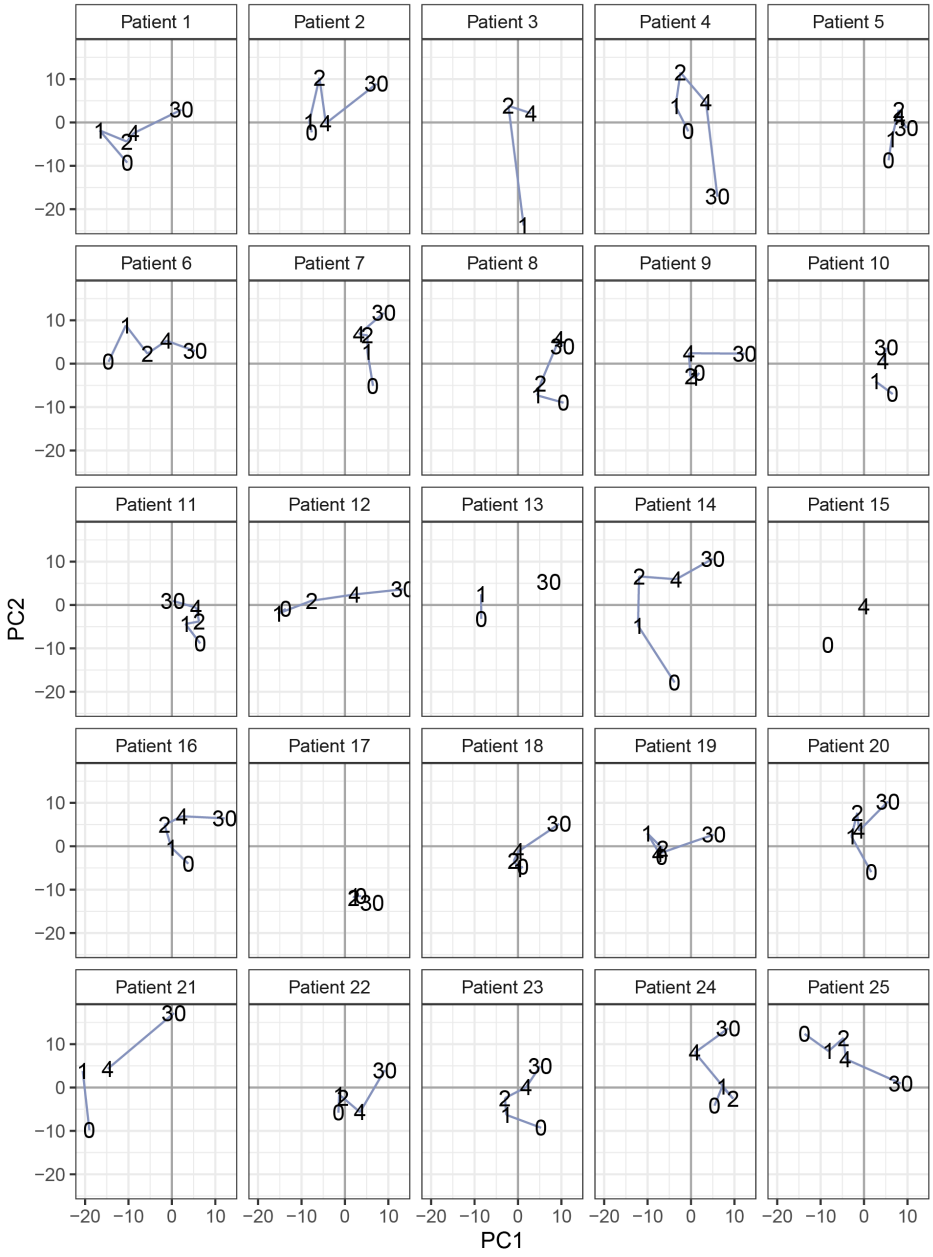

Figure 4.7 PCA score plots for each patient. For each patient, the time points are labelled and connected with lines. Abbreviations: PC: principal component

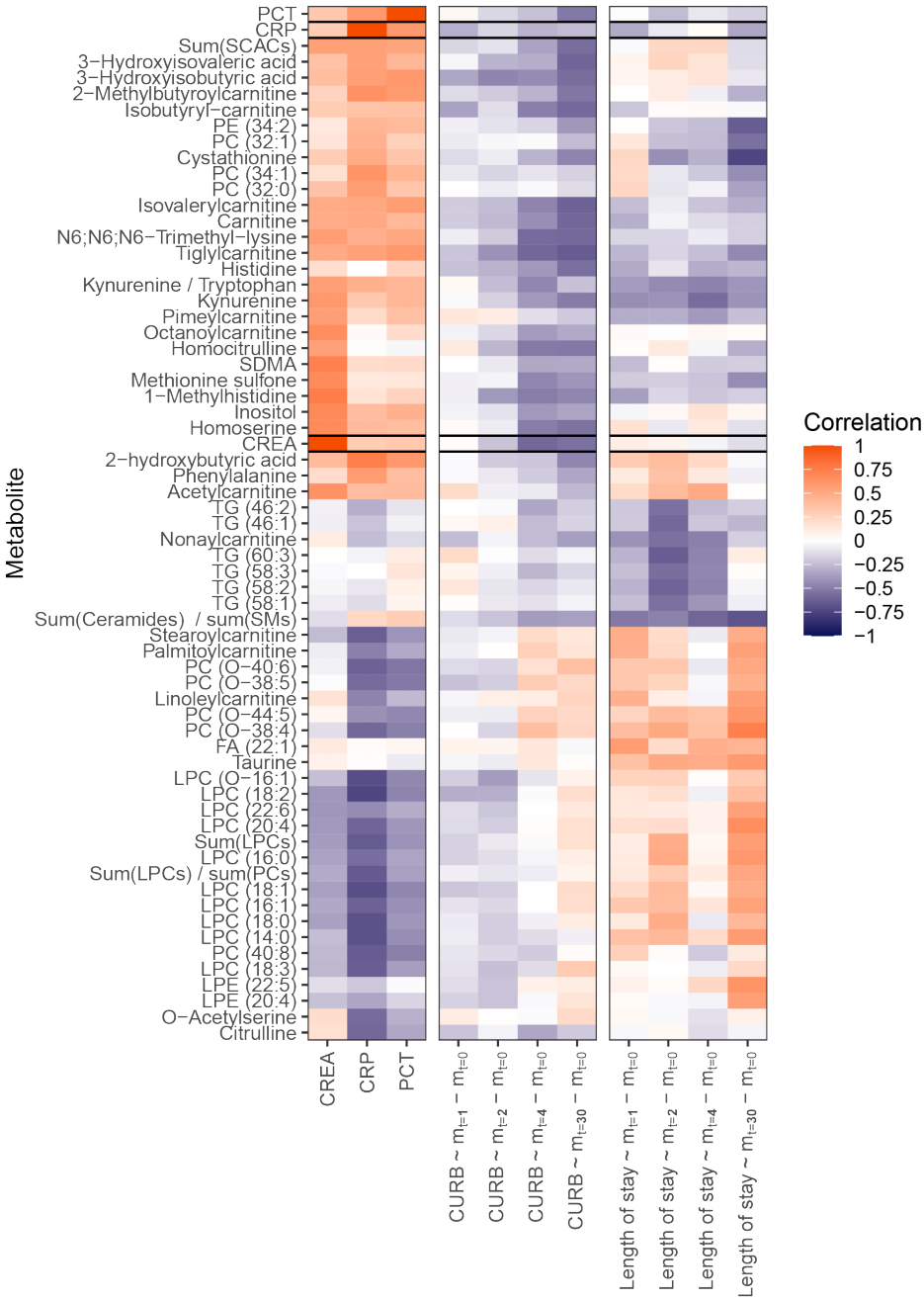

Figure 4.8 The correlations between metabolites and creatinine, CRP, and PCT over time; and the correlations of the CURB score and length of stay with a change of the metabolites between day k and day 0, where the change in metabolite levels is denoted by mt=k mt=0.

Table 4.2 Metabolite ratios and sums

Metabolite sum or ratio name in R	Metabolite sum or ratio formula
BCAA_sum	isoleucine + leucine + valine
TCA_cycle_sum	Citric acid + lactic acid + malic acid + fumaric acid
urea_cycle_sum	Citrulline + arginine + ornithine + fumaric acid
lc_Carnitines_sum	Myristoilcarnitine + Hexadecenoylcarntine + Palmitoylcarnitine + Stearoylcarnitine + Dodecenoylcarnitine + Tetradecenoylcarnitine + Linoleylcarnitine + Oleylcarnitine + Tetradecadienylcarntine
mc_Carnitines_sum	Hexanoylcarnitine + Octanoylcarnitine + Octenoylcarnitine + Decanoylcarnitine + Lauroylcarnitine + Nonaylcarnitine + Pimeylcarnitine + Decenoylcarnitine
sc_Carnitines_sum	Acetylcarnitine + Propionylcarnitine + Isobutyrylcarnitine + Butyrylcarnitine + Tiglylcarnitine + Methylbutyroylcarnitine + Isovalerylcarnitine
Cer_sum	Cer(d18:1/22:1) + Cer. (d18:1/24.1. + Cer(d18:1/24:0) + Cer(d18:1/16:0) + Cer(d18:1/23:0) + Cer(d18:1/24:0)
SM_sum	Sphingomyelin (d18:1/14:0) + (d18:1/15:0) + (d18:1/16:0) + (d18:1/16:1) + (d18:1/17:0) + (d18:1/18:0) + (d18:1/18:1) + (d18:1/18:2) + (d18:1/20:0) + (d18:1/20:1) + (d18:1/21:0) + (d18:1/22:0) + (d18:1/22:1) + (d18:1/23:0) + (d18:1/ 23:1) + (d18:0/24:0) + (d18:0/24:1) + (d18:0/24:2) + (d18:0/25:0) + (d18:0/25:1)
LPC_sum	Lysophosphatidylcholine (14:0) + (16:0) + (16:1) + (18:0) + (18:1) + (18:2) + (18:3) + (20:4) + (20:5) + (22:6) + (O-16:1) + (O-18:1)
PC_sum	Diacyl-phosphatidylcholine (32:0) + (32:1) + (32:2) + (34:1) + (34:2) + (34:3) + (34:4) + (36:1) + (36:2) + (36:3) + (36:4) + (36:5) + (36:6) + (38:2) + (38:3) + (38:4) + (38:5) + (38:6) + (38:7) + (40:4) + (40:5) + (40:6) + (40:7) + (40:8) + (O-34:1) + (O-34:2) + (O-34:3) + (O-36:2) + (O-36:3) + (O-36:4) + (O-36:5) + (O-36:6) + (O-38:4) + (O-38:5) + (O-38:6) + (O-38:7) + (O-40:6) + (O-42:6) + (O-44:5)
HT5_Trp_ratio	Serotonine / Tryptophan
ADMA_Arg_ratio	ADMA / Arginine
SDMA_Arg_ratio	SDMA / Arginine
Carnitine_sum_lc_Carnitines_ratio	Carnitine / LCAC sum
Carnitine_sum_mc_Carnitines_ratio	Carnitine / MCAC sum
Carnitine_sum_sc_Carnitines_ratio	Carnitine / SCAC sum
DCA_CA_ratio	DCA / CA
FA_14.1_14.0	FA (14:1) / FA (14:0)
FA_16.1_16.0	FA (16:1) / FA(16:0)
Gln_Glu	Glutamine / Glutamic acid
Kyn_Trp	Kynurenine / Tryptophan
sum_BCAA_sum_Phe_Tyr_ratio	BCAA sum / (Phenylalanine + Tyrosine)
sum_CER_sum_SM_ratio	Cer sum / SM sum
sum_LPC_sum_PC_ratio	LPC sum / PC sum

Table 4.3 Metabolite ratios and sums

Biochemical class	Metabolite	Biochemical class	Metabolite
Acylcarnitines	Acetylcarnitine	Betaines	Betaine
Acylcarnitines	Butyrylcarnitine	Bile acids and other steroids	Cholic acid
Acylcarnitines	Decanoylcarnitine	Bile acids and other steroids	Cortisol
Acylcarnitines	Decenoylcarnitine	Bile acids and other steroids	Deoxycholic acid
Acylcarnitines	Dodecanoylcarnitine	Bile acids and other steroids	GCA
Acylcarnitines	9-Hexadecenoylcarnitine	Bile acids and other steroids	GCDCA
Acylcarnitines	Hexanoylcarnitine	Bile acids and other steroids	GDCA
Acylcarnitines	Isobutyryl-carnitine	Bile acids and other steroids	GLCA
Acylcarnitines	Isovalerylcarnitine	Bile acids and other steroids	GUDCA
Acylcarnitines	Lauroylcarnitine	Bile acids and other steroids	TCA
Acylcarnitines	Linoleylcarnitine	Biogenic amines	ADMA
Acylcarnitines	Myristoylcarnitine	Biogenic amines	Anserine
Acylcarnitines	Nonaylcarnitine	Biogenic amines	Beta-Alanine
Acylcarnitines	2-Octenoylcarnitine	Biogenic amines	Cystathionine
Acylcarnitines	Octanoylcarnitine	Biogenic amines	3-Aminoisobutyric acid
Acylcarnitines	Oleylcarnitine	Biogenic amines	Ethanolamine
Acylcarnitines	Palmitoylcarnitine	Biogenic amines	N2-gamma-Glutamylglutamine
Acylcarnitines	Pimeylcarnitine	Biogenic amines	gamma-Glutamylalanine
Acylcarnitines	Propionylcarnitine	Biogenic amines	Glutathione
Acylcarnitines	Stearoylcarnitine	Biogenic amines	Glycylglycine
Acylcarnitines	Tetradecadienylcarntine	Biogenic amines	Glycylproline
Acylcarnitines	Tetradecanoylcarnitine	Biogenic amines	Homocitrulline
Acylcarnitines	Tiglylcarnitine	Biogenic amines	Homocysteine
Acylcarnitines	2-Methylbutyroylcarnitine	Biogenic amines	5-Hydroxylysine
Amino acids	Citrulline	Biogenic amines	Aminoadipic acid
Amino acids	Cysteine	Biogenic amines	Alpha-aminobutyric acid
Amino acids	Glycine	Biogenic amines	Homoserine
Amino acids	4-Hydroxyproline	Biogenic amines	Kynurenine
Amino acids	Alanine	Biogenic amines	Methionine sulfoxide
Amino acids	Arginine	Biogenic amines	Methionine sulfone
Amino acids	Asparagine	Biogenic amines	N6, N6, N6-Trimethyl-lysine
Amino acids	Aspartic acid	Biogenic amines	O-Acetylserine
Amino acids	Glutamic acid	Biogenic amines	Putrescine
Amino acids	Glutamine	Biogenic amines	Methylcysteine
Amino acids	Histidine	Biogenic amines	Saccharopine
Amino acids	Isoleucine	Biogenic amines	Sarcosine
Amino acids	Leucine	Biogenic amines	SDMA
Amino acids	Lysine	Biogenic amines	Serotonin
Amino acids	Methionine	Biogenic amines	Taurine
Amino acids	Phenylalanine	Biogenic amines	1-Methylhistidine
Amino acids	Proline	Biogenic amines	3-Methoxytyramine
Amino acids	Serine	Biogenic amines	5-Aminolevulinic acid
Amino acids	Threonine	Carnitines	Carnitine
Amino acids	Tryptophan	Ceramides	Ceramide (d18:0/24:0)
Amino acids	Tyrosine	Ceramides	Ceramide (d18:1/16:0)
Amino acids	Valine	Ceramides	Ceramide (d18:1/22:1)
Amino acids	Ornithine	Ceramides	Ceramide (d18:1/23:0)
		Ceramides	Ceramide (d18:1/24:0)
		Ceramides	Ceramide (d18:1/24:1)

Biochemical class	Metabolite	Biochemical class	Metabolite
Cholesteryl esters	CE (18:3)	Diacyl-phosphatidylethanolamine	PE (34:2)
Cholesteryl esters	CE (18:2)	Diacyl-phosphatidylethanolamine	PE (36:3)
Cholesteryl esters	CE (18:1)	Diacyl-phosphatidylethanolamine	PE (36:4)
Cholesteryl esters	CE (20:5)	Diacyl-phosphatidylethanolamine	PE (38:2)
Cholesteryl esters	CE (22:6)	Diacyl-phosphatidylethanolamine	PE (38:4)
Cholines	Choline	Diacyl-phosphatidylethanolamine	PE (38:6)
Diacylglycerols	DG (36:2)	Diacyl-phosphatidylethanolamine	PE (O-36:5)
Diacylglycerols	DG (36:3)	Diacyl-phosphatidylethanolamine	PE (O-38:5)
Diacylglycerols	DG (36:4)	Diacyl-phosphatidylethanolamine	PE (O-38:7)
Diacyl-phosphatidylcholine	PC (32:0)	Endocannabinoids	alpha-LEA
Diacyl-phosphatidylcholine	PC (32:1)	Endocannabinoids	AEA
Diacyl-phosphatidylcholine	PC (32:2)	Endocannabinoids	DEA
Diacyl-phosphatidylcholine	PC (34:1)	Endocannabinoids	DGLEA
Diacyl-phosphatidylcholine	PC (34:2)	Endocannabinoids	DHEA
Diacyl-phosphatidylcholine	PC (34:3)	Endocannabinoids	LEA
Diacyl-phosphatidylcholine	PC (34:4)	Endocannabinoids	O-AEA
Diacyl-phosphatidylcholine	PC (36:1)	Endocannabinoids	PEA
Diacyl-phosphatidylcholine	PC (36:2)	Endocannabinoids	POEA
Diacyl-phosphatidylcholine	PC (36:3)	Endocannabinoids	SEA
Diacyl-phosphatidylcholine	PC (36:4)	Endocannabinoids	1-/2-Arachidonoyl Glycerol (20:4)
Diacyl-phosphatidylcholine	PC (36:5)	Endocannabinoids	1-Linoleoyl Glycerol (18:2)
Diacyl-phosphatidylcholine	PC (36:6)	Fatty acids	FA (14:0)
Diacyl-phosphatidylcholine	PC (38:2)	Fatty acids	FA (14:1)
Diacyl-phosphatidylcholine	PC (38:3)	Fatty acids	FA (15:0)
Diacyl-phosphatidylcholine	PC (38:4)	Fatty acids	FA (16:0)
Diacyl-phosphatidylcholine	PC (38:5)	Fatty acids	FA (16:1)
Diacyl-phosphatidylcholine	PC (38:6)	Fatty acids	FA (17:0)
Diacyl-phosphatidylcholine	PC (38:7)	Fatty acids	FA (17:1)
Diacyl-phosphatidylcholine	PC (40:4)	Fatty acids	FA (18:1)
Diacyl-phosphatidylcholine	PC (40:5)	Fatty acids	FA (20:0)
Diacyl-phosphatidylcholine	PC (40:6)	Fatty acids	FA (20:1)
Diacyl-phosphatidylcholine	PC (40:7)	Fatty acids	FA (20:2)
Diacyl-phosphatidylcholine	PC (40:8)	Fatty acids	FA (22:1)
Diacyl-phosphatidylcholine	PC (O-34:1)	Fatty acids	FA (22:4)
Diacyl-phosphatidylcholine	PC (O-34:2)	Fatty acids	FA (22:5)-w6
Diacyl-phosphatidylcholine	PC (O-34:3)	Fatty acids	FA (22:6)
Diacyl-phosphatidylcholine	PC (O-36:2)	Fatty acids	FA (24:1)
Diacyl-phosphatidylcholine	PC (O-36:3)	Free fatty acids	FA (18:1)
Diacyl-phosphatidylcholine	PC (O-36:4)	Free fatty acids	FA (18:2)
Diacyl-phosphatidylcholine	PC (O-36:5)	Free fatty acids	FA (20:5)
Diacyl-phosphatidylcholine	PC (O-36:6)	Free fatty acids	FA (22:4)-w6
Diacyl-phosphatidylcholine	PC (O-38:4)	Free fatty acids	FA (22:5)-w3
Diacyl-phosphatidylcholine	PC (O-38:5)	Free fatty acids	FA (22:5)-w6
Diacyl-phosphatidylcholine	PC (O-38:6)	Free fatty acids	FA (22:6)
Diacyl-phosphatidylcholine	PC (O-38:7)		
Diacyl-phosphatidylcholine	PC (O-40:6)		
Diacyl-phosphatidylcholine	PC (O-42:6)		
Diacyl-phosphatidylcholine	PC (O-44:5)		

Biochemical class	Metabolite	Biochemical class	Metabolite
Lysophosphatidylcholine	LPC (14:0)	Lysophospholipids	LPS (18:0)
Lysophosphatidylcholine	LPC (16:0)	Lysophospholipids	LPS (18:1)
Lysophosphatidylcholine	LPC (16:1)	Lysophospholipids	LPS (20:4)
Lysophosphatidylcholine	LPC (18:0)	Lysophospholipids	LPS (22:4)
Lysophosphatidylcholine	LPC (18:1)	Lysophospholipids	LPS (22:6)
Lysophosphatidylcholine	LPC (18:2)	Nitro-Fatty Acids	10-NO2(OA9)NO2(OA)
Lysophosphatidylcholine	LPC (18:3)	Organic acids	Inositol
Lysophosphatidylcholine	LPC (20:4)	Organic acids	2-hydroxybutyric acid
Lysophosphatidylcholine	LPC (20:5)	Organic acids	Citric acid
Lysophosphatidylcholine	LPC (22:6)	Organic acids	Glutamic acid
Lysophosphatidylcholine	LPC (O-16:1)	Organic acids	Lactic acid
Lysophosphatidylcholine	LPC (O-18:1)	Organic acids	Malic acid
Lysophosphatidylethanolamines	LPE(22:6)	Organic acids	Fumaric acid
Lysophospholipids	LPA (14:0)	Organic acids	Pyroglutamic acid
Lysophospholipids	LPA (16:0)	Organic acids	3-Hydroxybutyric acid
Lysophospholipids	LPA (16:1)	Organic acids	Aspartic acid
Lysophospholipids	LPA (18:0)	Organic acids	3-Hydroxyisobutyric acid
Lysophospholipids	LPA (18:1)	Organic acids	3-Hydroxyisovaleric acid
Lysophospholipids	LPA (18:2)	Organic acids	Uracil
Lysophospholipids	LPA (20:3)	Oxylipins	PGF2a
Lysophospholipids	LPA (20:4)	Oxylipins	TXB2
Lysophospholipids	LPA (20:5)	Oxylipins	10-HDoHE
Lysophospholipids	LPA (22:4)	Oxylipins	11,12-DiHETrE
Lysophospholipids	LPA (22:6)	Oxylipins	11-HETE
Lysophospholipids	LPE (14:0)	Oxylipins	12,13-DiHODE
Lysophospholipids	LPE (16:0)	Oxylipins	12,13-DiHOME
Lysophospholipids	LPE (16:1)	Oxylipins	12-HETE
Lysophospholipids	LPE (18:0)	Oxylipins	12S-HEPE
Lysophospholipids	LPE (18:1)	Oxylipins	12S-HHTrE
Lysophospholipids	LPE (18:2)	Oxylipins	13-HODE
Lysophospholipids	LPE (20:3)	Oxylipins	14,15-DiHETrE
Lysophospholipids	LPE (20:4)	Oxylipins	14-HDoHE
Lysophospholipids	LPE (20:5)	Oxylipins	15-HETE
Lysophospholipids	LPE (22:4)	Oxylipins	15S-HETrE
Lysophospholipids	LPE (22:5)	Oxylipins	16-HDoHE
Lysophospholipids	LPE (22:6)	Oxylipins	17,18-DiHETE
Lysophospholipids	LPG (16:0)	Oxylipins	19,20-EpDPE
Lysophospholipids	LPG (16:1)	Oxylipins	19,20-DiHDPA
Lysophospholipids	LPG (18:0)	Oxylipins	20-HETE
Lysophospholipids	LPG (18:1)	Oxylipins	5,6-DiHETrE
Lysophospholipids	LPG (18:2)	Oxylipins	5-HETE
Lysophospholipids	LPG (20:3)	Oxylipins	5S-HEPE
Lysophospholipids	LPG (20:4)	Oxylipins	8,9-DiHETrE
Lysophospholipids	LPI (16:0)	Oxylipins	8-HETE
Lysophospholipids	LPI (16:1)	Oxylipins	9,10,13-TriHOME
Lysophospholipids	LPI (18:0)	Oxylipins	9,10-DiHOME
Lysophospholipids	LPI (18:1)	Oxylipins	9,12,13-TriHOME
Lysophospholipids	LPI (20:4)	Oxylipins	9-HODE
Lysophospholipids	LPI (22:4)	Oxylipins	9-HOTrE
Lysophospholipids	LPS (16:0)	Platelet activating factor	PAF(18:2)-adduct

Biochemical class	Metabolite	Biochemical class	Metabolite
Sphingolipids	S1P (16:1)	Triglycerides	TG (54:1)
Sphingolipids	S1P (18:0)	Triglycerides	TG (54:2)
Sphingolipids	S1P (18:1)	Triglycerides	TG (54:3)
Sphingolipids	S1P (18:2)	Triglycerides	TG (54:4)
Sphingomyelin	SM (d18:1/14:0)	Triglycerides	TG (54:5)
Sphingomyelin	SM (d18:1/15:0)	Triglycerides	TG (54:6)
Sphingomyelin	SM (d18:1/16:0)	Triglycerides	TG (54:7)
Sphingomyelin	SM (d18:1/16:1)	Triglycerides	TG (55:2)
Sphingomyelin	SM (d18:1/17:0)	Triglycerides	TG (55:3)
Sphingomyelin	SM (d18:1/18:0)	Triglycerides	TG (56:2)
Sphingomyelin	SM (d18:1/18:1)	Triglycerides	TG (56:3)
Sphingomyelin	SM (d18:1/18:2)	Triglycerides	TG (56:4)
Sphingomyelin	SM (d18:1/20:0)	Triglycerides	TG (56:5)
Sphingomyelin	SM (d18:1/20:1)	Triglycerides	TG (56:6)
Sphingomyelin	SM (d18:1/21:0)	Triglycerides	TG (56:7)
Sphingomyelin	SM (d18:1/22:0)	Triglycerides	TG (55:1)
Sphingomyelin	SM (d18:1/22:1)	Triglycerides	TG (58:1)
Sphingomyelin	SM (d18:1/23:0)	Triglycerides	TG (58:10)
Sphingomyelin	SM (d18:1/ 23:1)	Triglycerides	TG (58:2)
Sphingomyelin	SM (d18:0/24:0)	Triglycerides	TG (58:3)
Sphingomyelin	SM (d18:0/24:1)	Triglycerides	TG (58:4)
Sphingomyelin	SM (d18:0/24:2)	Triglycerides	TG (58:5)
Sphingomyelin	SM (d18:0/25:0)	Triglycerides	TG (58:6)
Sphingomyelin	SM (d18:0/25:1)	Triglycerides	TG (58:8)
Triglycerides	TG (44:2)	Triglycerides	TG (58:9)
Triglycerides	TG (46:1)	Triglycerides	TG (60:2)
Triglycerides	TG (46:2)	Triglycerides	TG (60:3)
Triglycerides	TG (48:0)	Trimethylamine-N-oxides	TMAO
Triglycerides	TG (48:1)		
Triglycerides	TG (48:2)		
Triglycerides	TG (48:3)		
Triglycerides	TG (O-50:2)		
Triglycerides	TG (50:1)		
Triglycerides	TG (50:2)		
Triglycerides	TG (50:3)		
Triglycerides	TG (50:4)		
Triglycerides	TG (51:1)		
Triglycerides	TG (51:2)		
Triglycerides	TG (51:3)		
Triglycerides	TG (51:4)		
Triglycerides	TG (52:1)		
Triglycerides	TG (52:2)		
Triglycerides	TG (52:3)		
Triglycerides	TG (52:4)		
Triglycerides	TG (52:5)		
Triglycerides	TG (52:6)		
Triglycerides	TG (53:1)		